

000  
 001  
 002  
 003  
 004 **Supplementary Material to “External Prior Guided Internal Prior Learning for**  
 005 **Real Noisy Image Denoising”**  
 006  
 007  
 008  
 009  
 010  
 011  
 012  
 013  
 014  
 015  
 016  
 017  
 018  
 019  
 020  
 021  
 022  
 023  
 024  
 025  
 026  
 027  
 028  
 029  
 030  
 031  
 032  
 033  
 034  
 035  
 036  
 037  
 038  
 039  
 040  
 041  
 042  
 043  
 044  
 045  
 046  
 047  
 048  
 049  
 050  
 051  
 052  
 053

054  
 055  
 056  
 057  
 058  
 059  
 060  
 061  
 062  
 063  
 064  
 065  
 066  
 067  
 068  
 069  
 070  
 071  
 072  
 073  
 074  
 075  
 076  
 077  
 078  
 079  
 080  
 081  
 082  
 083  
 084  
 085  
 086  
 087  
 088  
 089  
 090  
 091  
 092  
 093  
 094  
 095  
 096  
 097  
 098  
 099  
 100  
 101  
 102  
 103  
 104  
 105  
 106  
 107

Anonymous CVPR submission

Paper ID 1047

In this supplementary material, we provide:

1. The closed-form solution of the proposed weighted sparse coding model in the main paper.
2. More denoising results on the real noisy images (with no “ground truth”) provided in the dataset [1].
3. More denoising results on the 15 cropped real noisy images (with “ground truth”) used in the dataset [2].
4. More denoising results on the 60 cropped real noisy images (with “ground truth”) from [2].

## 1. Closed-Form Solution of the Weighted Sparse Coding Problem (4)

The weighted sparse coding problem in the main paper is:

$$\min_{\alpha} \|\mathbf{y} - \mathbf{D}\alpha\|_2^2 + \|\mathbf{w}^T \alpha\|_1. \quad (1)$$

Since  $\mathbf{D}$  is an orthonormal matrix, problem (1) is equivalent to

$$\min_{\alpha} \|\mathbf{D}^T \mathbf{y} - \alpha\|_2^2 + \|\mathbf{w}^T \alpha\|_1. \quad (2)$$

For simplicity, we denote  $\mathbf{z} = \mathbf{D}^T \mathbf{y}$ . Since  $\mathbf{w}_i = c * 2\sqrt{2}\sigma^2 / (\Lambda_i + \varepsilon)$  is positive (please refer to Eq. (18) in the main paper), problem (2) can be written as

$$\min_{\alpha} \sum_{i=1}^{p^2} ((\mathbf{z}_i - \alpha_i)^2 + \mathbf{w}_i |\alpha_i|). \quad (3)$$

The problem (3) is separable w.r.t.  $\alpha_i$  and can be simplified to  $p^2$  scalar minimization problems

$$\min_{\alpha_i} (\mathbf{z}_i - \alpha_i)^2 + \mathbf{w}_i |\alpha_i|, \quad (4)$$

where  $i = 1, \dots, p^2$ . Taking derivative of  $\alpha_i$  in problem (4) and setting the derivative to be zero. There are two cases for the solution.

(a) If  $\alpha_i \geq 0$ , we have

$$2(\alpha_i - \mathbf{z}_i) + \mathbf{w}_i = 0. \quad (5)$$

The solution is

$$\hat{\alpha}_i = \mathbf{z}_i - \frac{\mathbf{w}_i}{2} \geq 0. \quad (6)$$

So  $\mathbf{z}_i \geq \frac{\mathbf{w}_i}{2} > 0$ , and the solution  $\hat{\alpha}_i$  can be written as

$$\hat{\alpha}_i = \text{sgn}(\mathbf{z}_i) * (|\mathbf{z}_i| - \frac{\mathbf{w}_i}{2}), \quad (7)$$

where  $\text{sgn}(\bullet)$  is the sign function.

(b) If  $\alpha_i < 0$ , we have

$$2(\alpha_i - \mathbf{z}_i) - \mathbf{w}_i = 0. \quad (8)$$

The solution is

$$\hat{\alpha}_i = \mathbf{z}_i + \frac{\mathbf{w}_i}{2} < 0. \quad (9)$$

So  $\mathbf{z}_i < -\frac{\mathbf{w}_i}{2} < 0$ , and the solution  $\hat{\alpha}_i$  can be written as

$$\hat{\alpha}_i = \text{sgn}(\mathbf{z}_i) * (-\mathbf{z}_i - \frac{\mathbf{w}_i}{2}) = \text{sgn}(\mathbf{z}_i) * (|\mathbf{z}_i| - \frac{\mathbf{w}_i}{2}). \quad (10)$$

108 In summary, we have the final solution of the weighted sparse coding problem (1) as 162  
 109  $\hat{\alpha} = \text{sgn}(\mathbf{D}^T \mathbf{y}) \odot \max(|\mathbf{D}^T \mathbf{y}| - \mathbf{w}/2, 0),$  163  
 110 where  $\odot$  means element-wise multiplication and  $|\mathbf{D}^T \mathbf{y}|$  is the absolute value of each entry of the vector  $\mathbf{D}^T \mathbf{y}.$  164  
 111  
 112 **2. More Results on Real Noisy Images in [1]** 165  
 113  
 114 In this section, we give more visual comparisons of the competing methods on the real noisy images provided in [1]. The 166  
 115 real noisy images in this dataset [1] have no “ground truth” images and hence we only compare the visual quality of the 167  
 116 denoised images by different methods. As can be seen from Figures 1-4, our proposed method performs better than the state- 168  
 117-of-the-art denoising methods. This validates the effectiveness of our proposed external prior guided internal prior learning 169  
 118 framework for real noisy image denoising. 170  
 119  
 120  
 121  
 122  
 123  
 124  
 125  
 126  
 127  
 128  
 129  
 130  
 131  
 132  
 133  
 134  
 135  
 136  
 137  
 138  
 139  
 140  
 141  
 142  
 143  
 144  
 145  
 146  
 147  
 148  
 149  
 150  
 151  
 152  
 153  
 154  
 155  
 156  
 157  
 158  
 159  
 160  
 161

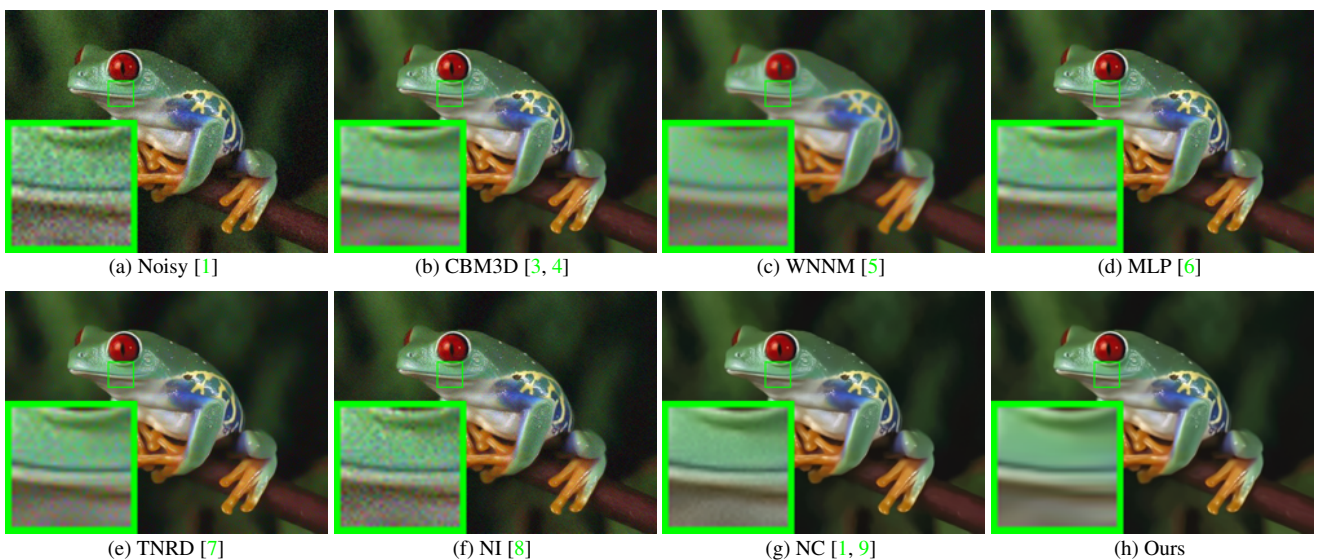


Figure 1. Denoised images of the real noisy image “Frog” [1] by different methods. The images are better to be zoomed in on screen.

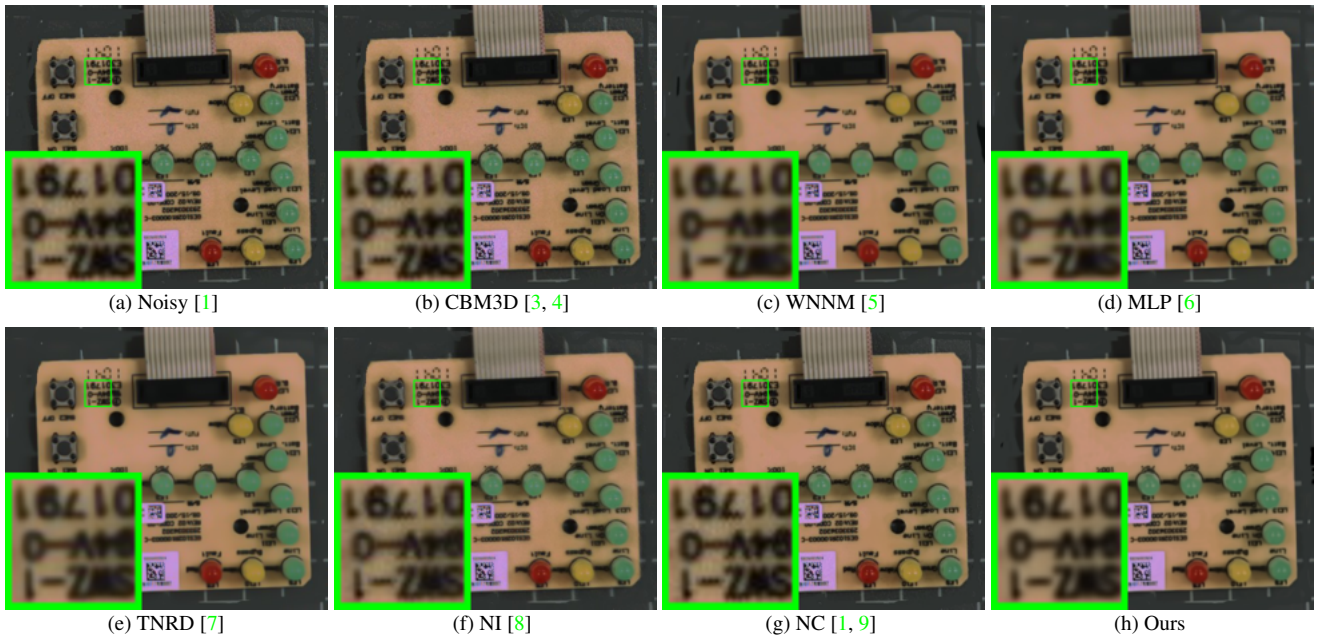


Figure 2. Denoised images of the real noisy image “Circuit” [1] by different methods. The images are better to be zoomed in on screen.



Figure 3. Denoised images of the real noisy image “Woman” [1] by different methods. The images are better to be zoomed in on screen.

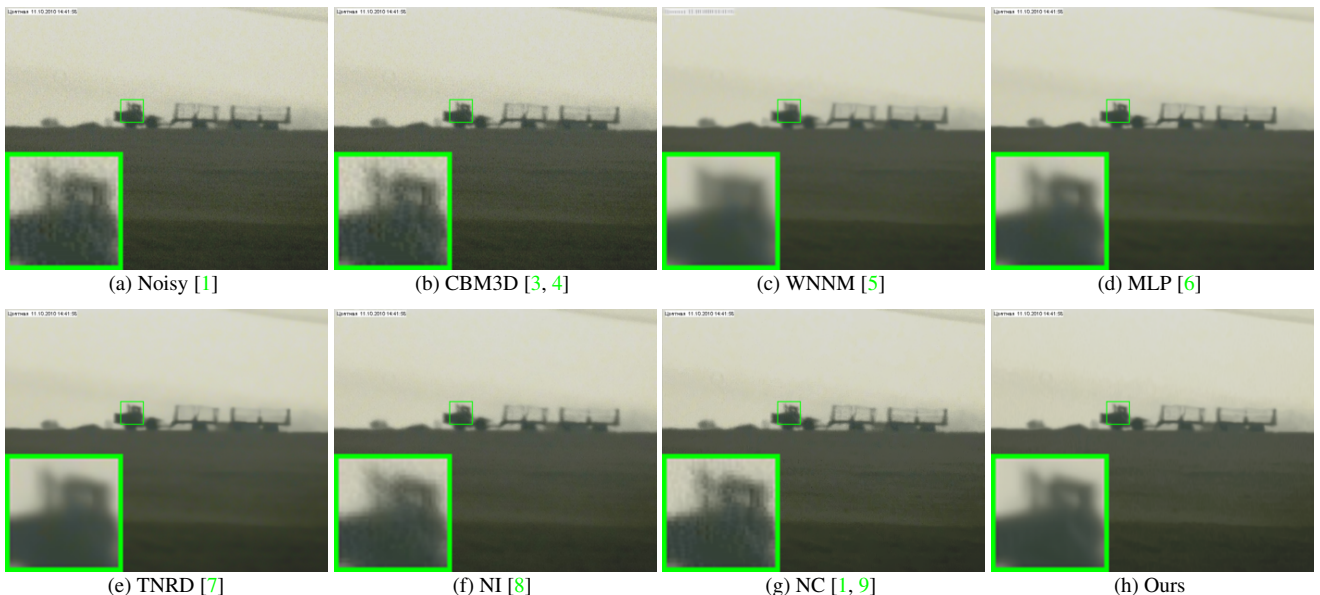


Figure 4. Denoised images of the real noisy image “Vehicle” [1] by different methods. The images are better to be zoomed in on screen.

### 3. More Results on the 15 Cropped Images Used in [2]

In this section, we provide more visual comparisons of the proposed method with the state-of-the-art denoising methods on the 15 cropped real noisy images used in [2]. As can be seen from Figures 5-9, on most cases, our proposed method achieves better performance than the competing methods. This validates the effectiveness of our proposed external prior guided internal prior learning framework for real noisy image denoising.

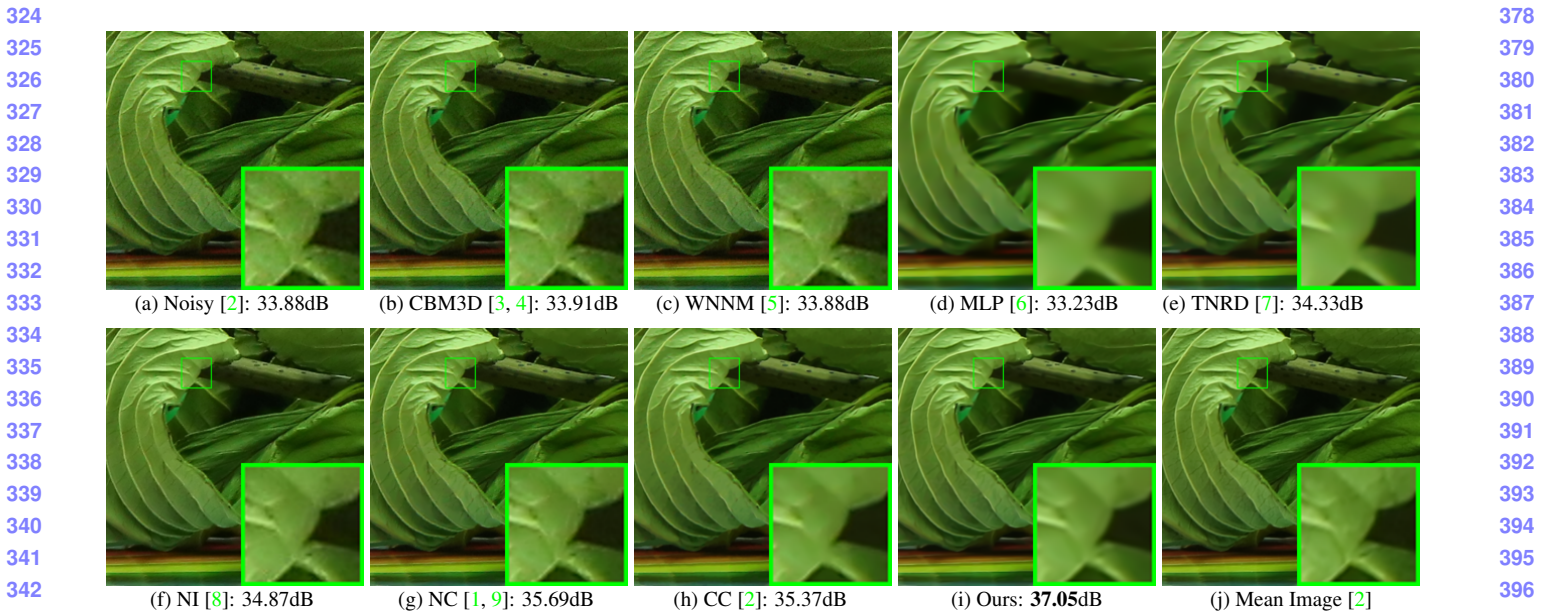


Figure 5. Denoised images of a region cropped from the real noisy image “Canon 5D Mark 3 ISO 3200 2” [2] by different methods. The images are better to be zoomed in on screen.

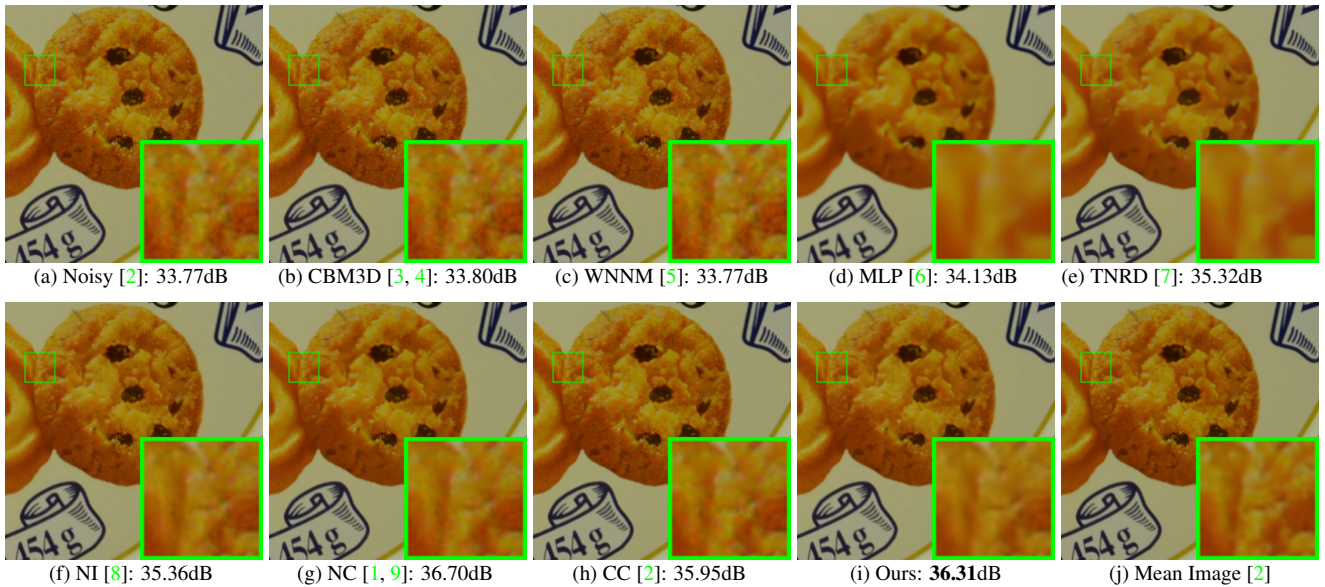


Figure 6. Denoised images of a region cropped from the real noisy image “Canon 5D Mark 3 ISO 3200 2” [2] by different methods. The images are better to be zoomed in on screen.

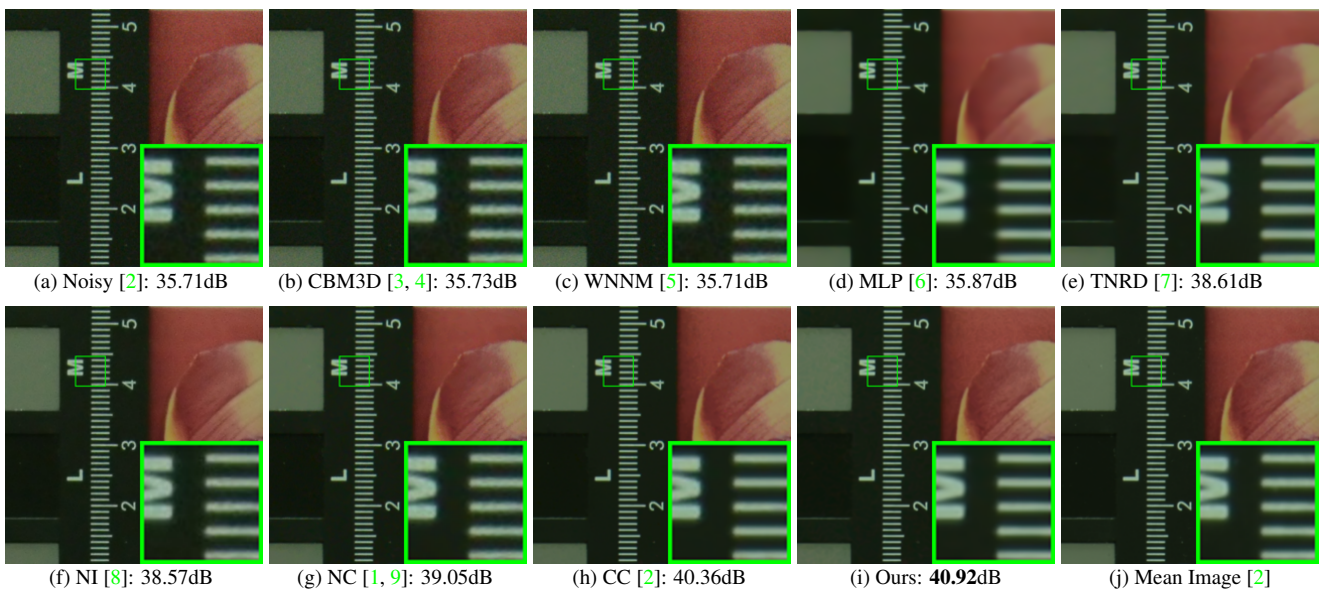


Figure 7. Denoised images of a region cropped from the real noisy image “Nikon D800 ISO 1600 2” [2] by different methods. The images are better to be zoomed in on screen.

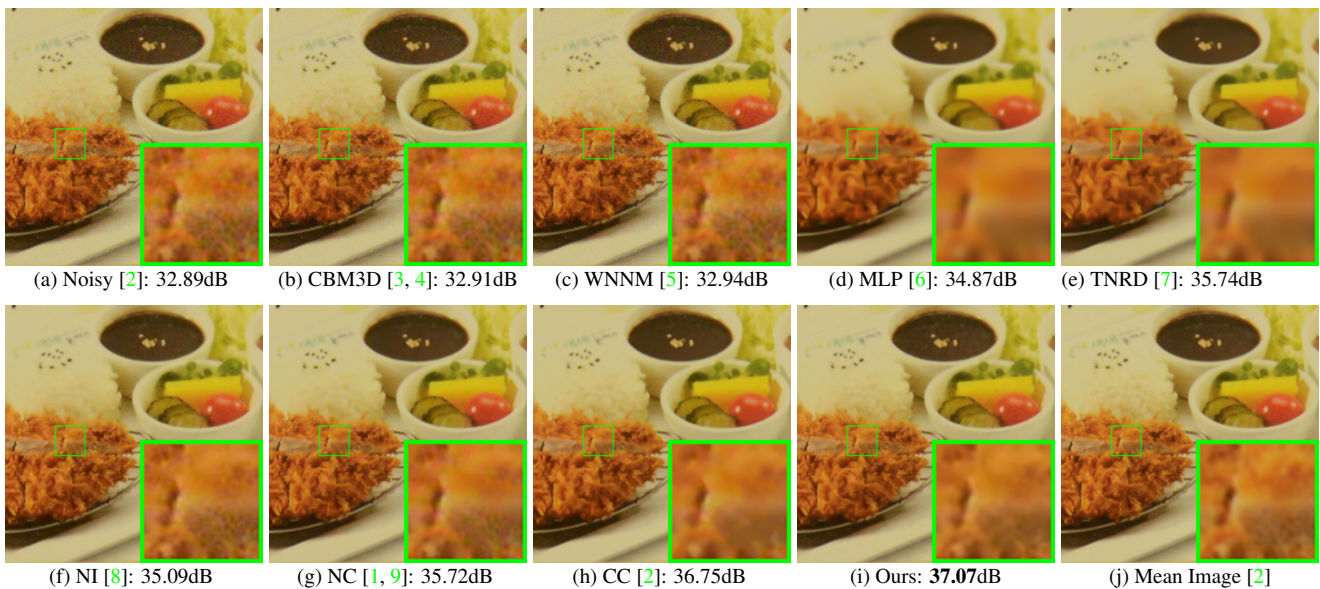


Figure 8. Denoised images of a region cropped from the real noisy image “Nikon D800 ISO 3200 2” [2] by different methods. The images are better to be zoomed in on screen.

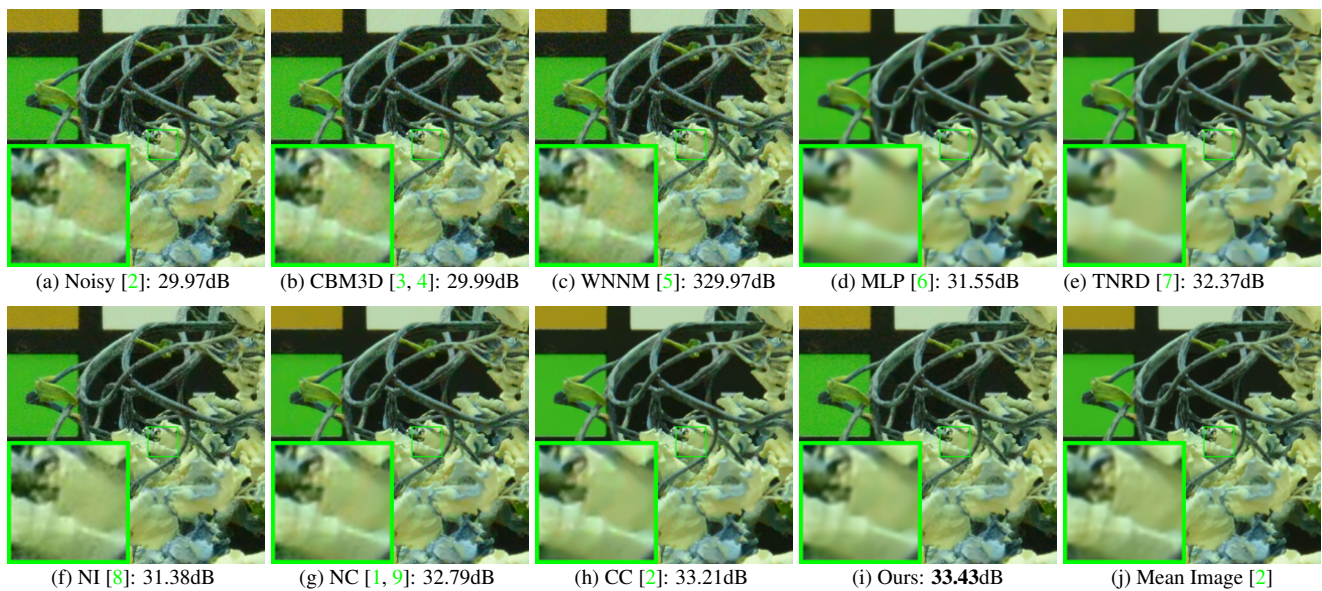


Figure 9. Denoised images of a region cropped from the real noisy image “Nikon D800 ISO 6400 2” [2] by different methods. The images are better to be zoomed in on screen.

#### 4. More Results on the 60 Cropped Images in [2]

In this section, we provide more visual comparisons of the proposed method with the state-of-the-art denoising methods on the 60 cropped real noisy images we cropped from [2]. As can be seen from Figures 11-??, on most cases, our proposed method achieves better performance than the competing methods. This validates the effectiveness of our proposed external prior guided internal prior learning framework for real noisy image denoising.

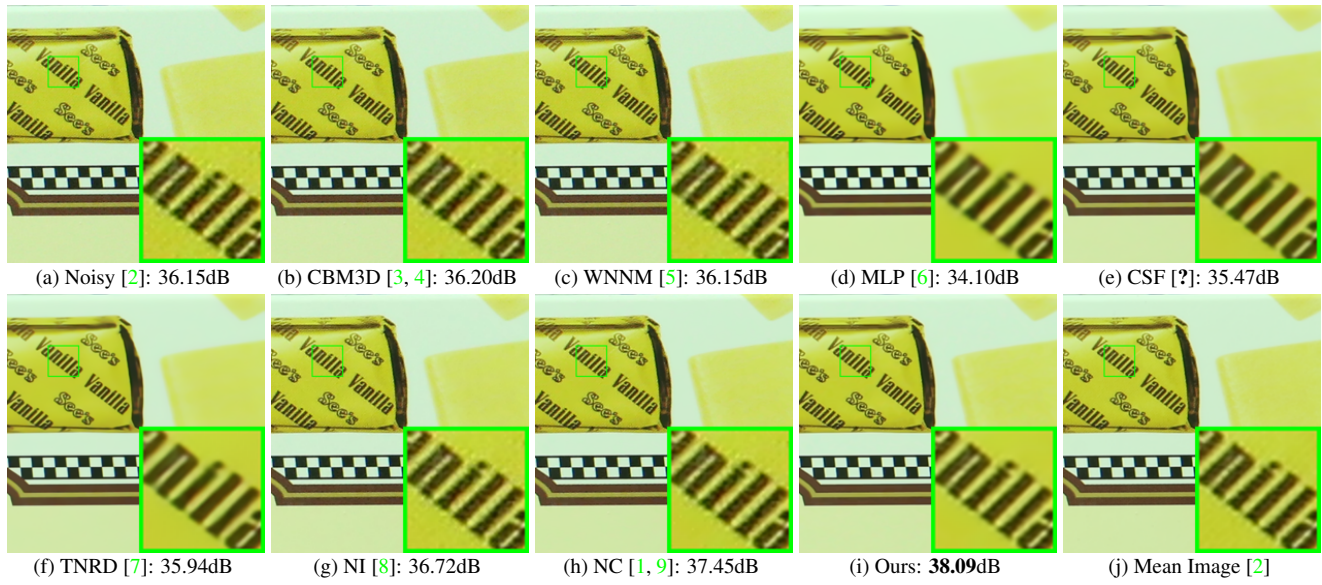


Figure 10. Denoised images of a region cropped from the real noisy image “Canon EOS 5D Mark3 ISO 3200 C1” [2] by different methods. The images are better viewed by zooming in on screen.

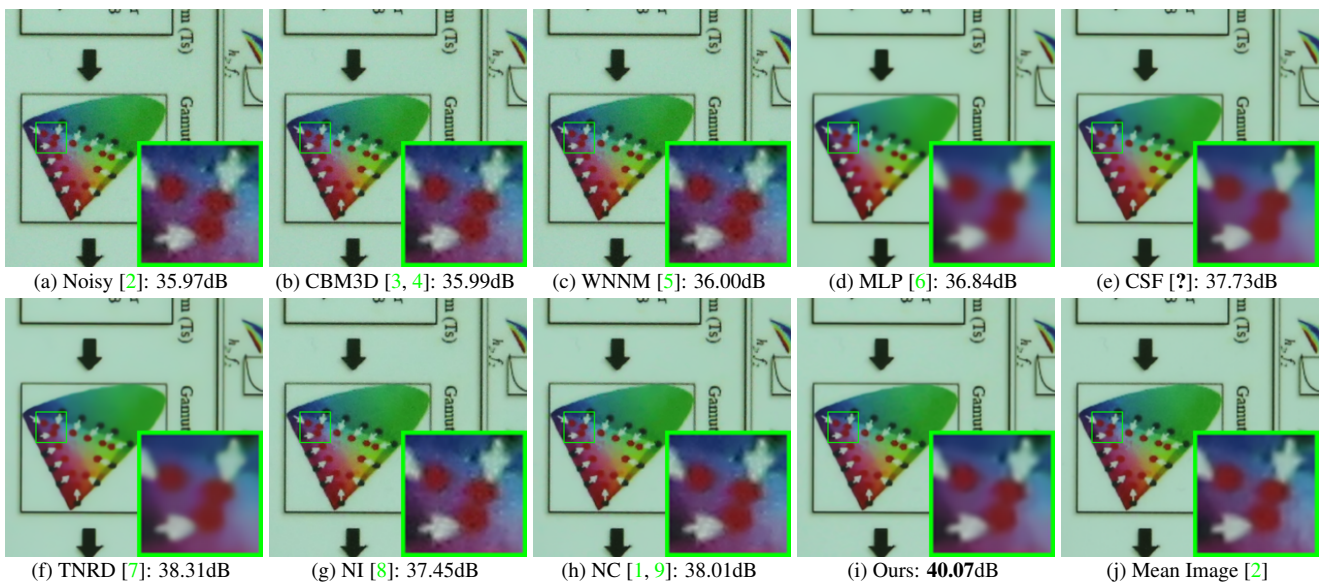


Figure 11. Denoised imagesupp of a region cropped from the real noisy image “Canon EOS 5D Mark3 ISO 3200 C2” [2] by different methods. The images are better viewed by zooming in on screen.

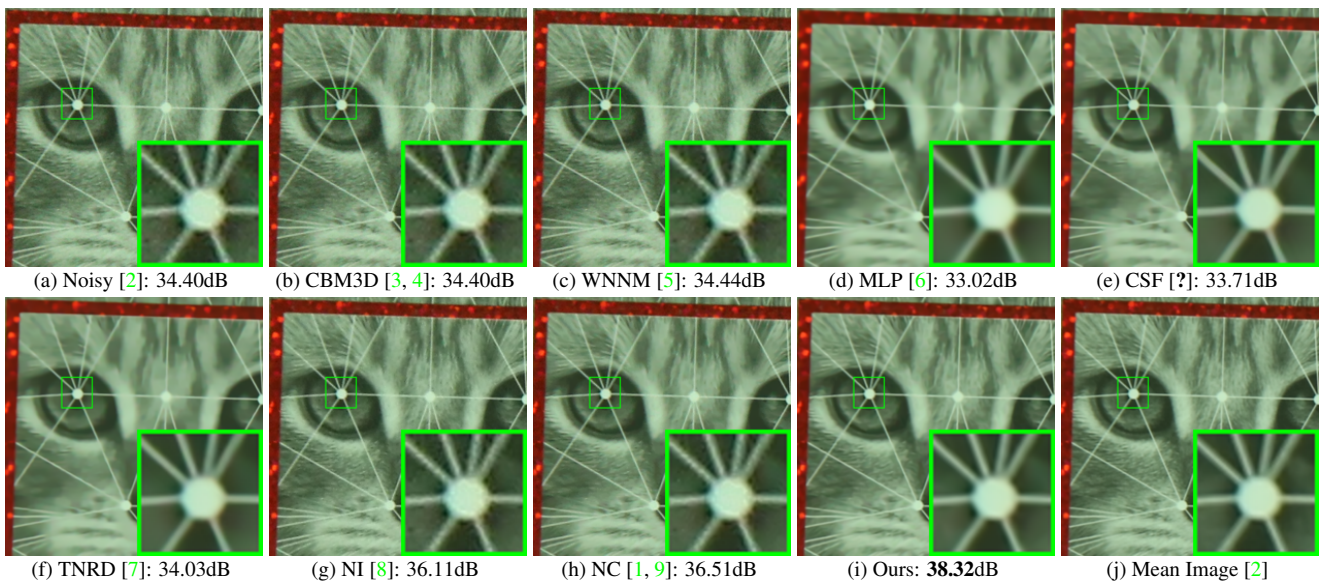


Figure 12. Denoised imagesupp of a region cropped from the real noisy image “Canon EOS 5D Mark3 ISO 3200 C3” [2] by different methods. The images are better viewed by zooming in on screen.

## References

- [1] M. Lebrun, M. Colom, and J. M. Morel. The noise clinic: a blind image denoising algorithm. <http://www.ipol.im/pub/art/2015/125/>. Accessed 01 28, 2015. 1, 2, 3, 4, 5, 6, 7
- [2] S. Nam, Y. Hwang, Y. Matsushita, and S. J. Kim. A holistic approach to cross-channel image noise modeling and its application to image denoising. *IEEE Conference on Computer Vision and Pattern Recognition (CVPR)*, pages 1683–1691, 2016. 1, 3, 4, 5, 6, 7
- [3] K. Dabov, A. Foi, V. Katkovnik, and K. Egiazarian. Image denoising by sparse 3-D transform-domain collaborative filtering. *IEEE Transactions on Image Processing*, 16(8):2080–2095, 2007. 2, 3, 4, 5, 6, 7

- 756 [4] K. Dabov, A. Foi, V. Katkovnik, and K. Egiazarian. Color image denoising via sparse 3D collaborative filtering with grouping  
757 constraint in luminance-chrominance space. *IEEE International Conference on Image Processing (ICIP)*, pages 313–316, 2007. 2, 3,  
758 4, 5, 6, 7 810  
759 [5] S. Gu, L. Zhang, W. Zuo, and X. Feng. Weighted nuclear norm minimization with application to image denoising. *IEEE Conference*  
760 *on Computer Vision and Pattern Recognition (CVPR)*, pages 2862–2869, 2014. 2, 3, 4, 5, 6, 7 811  
761 [6] H. C. Burger, C. J. Schuler, and S. Harmeling. Image denoising: Can plain neural networks compete with BM3D? *IEEE Conference*  
762 *on Computer Vision and Pattern Recognition (CVPR)*, pages 2392–2399, 2012. 2, 3, 4, 5, 6, 7 812  
763 [7] Y. Chen, W. Yu, and T. Pock. On learning optimized reaction diffusion processes for effective image restoration. *IEEE Conference on*  
764 *Computer Vision and Pattern Recognition (CVPR)*, pages 5261–5269, 2015. 2, 3, 4, 5, 6, 7 813  
765 [8] Neatlab ABSoft. Neat Image. <https://ni.neatvideo.com/home>. 2, 3, 4, 5, 6, 7 814  
766 [9] M. Lebrun, M. Colom, and J.-M. Morel. Multiscale image blind denoising. *IEEE Transactions on Image Processing*, 24(10):3149–  
767 3161, 2015. 2, 3, 4, 5, 6, 7 815  
768 [10] M. Elad, A. Bruckstein, and M. Aharon. Sparse representation for image restoration. *IEEE Transactions on Image Processing*, 15(12):3737–  
769 3748, 2006. 2, 3, 4, 5, 6, 7 816  
770 [11] M. Elad, M. Aharon, and A. Bruckstein. Sparse representation for image restoration. *IEEE Transactions on Image Processing*, 15(12):3737–  
771 3748, 2006. 2, 3, 4, 5, 6, 7 817  
772 [12] M. Elad, M. Aharon, and A. Bruckstein. Sparse representation for image restoration. *IEEE Transactions on Image Processing*, 15(12):3737–  
773 3748, 2006. 2, 3, 4, 5, 6, 7 818  
774 [13] M. Elad, M. Aharon, and A. Bruckstein. Sparse representation for image restoration. *IEEE Transactions on Image Processing*, 15(12):3737–  
775 3748, 2006. 2, 3, 4, 5, 6, 7 819  
776 [14] M. Elad, M. Aharon, and A. Bruckstein. Sparse representation for image restoration. *IEEE Transactions on Image Processing*, 15(12):3737–  
777 3748, 2006. 2, 3, 4, 5, 6, 7 820  
778 [15] M. Elad, M. Aharon, and A. Bruckstein. Sparse representation for image restoration. *IEEE Transactions on Image Processing*, 15(12):3737–  
779 3748, 2006. 2, 3, 4, 5, 6, 7 821  
780 [16] M. Elad, M. Aharon, and A. Bruckstein. Sparse representation for image restoration. *IEEE Transactions on Image Processing*, 15(12):3737–  
781 3748, 2006. 2, 3, 4, 5, 6, 7 822  
782 [17] M. Elad, M. Aharon, and A. Bruckstein. Sparse representation for image restoration. *IEEE Transactions on Image Processing*, 15(12):3737–  
783 3748, 2006. 2, 3, 4, 5, 6, 7 823  
784 [18] M. Elad, M. Aharon, and A. Bruckstein. Sparse representation for image restoration. *IEEE Transactions on Image Processing*, 15(12):3737–  
785 3748, 2006. 2, 3, 4, 5, 6, 7 824  
786 [19] M. Elad, M. Aharon, and A. Bruckstein. Sparse representation for image restoration. *IEEE Transactions on Image Processing*, 15(12):3737–  
787 3748, 2006. 2, 3, 4, 5, 6, 7 825  
788 [20] M. Elad, M. Aharon, and A. Bruckstein. Sparse representation for image restoration. *IEEE Transactions on Image Processing*, 15(12):3737–  
789 3748, 2006. 2, 3, 4, 5, 6, 7 826  
790 [21] M. Elad, M. Aharon, and A. Bruckstein. Sparse representation for image restoration. *IEEE Transactions on Image Processing*, 15(12):3737–  
791 3748, 2006. 2, 3, 4, 5, 6, 7 827  
792 [22] M. Elad, M. Aharon, and A. Bruckstein. Sparse representation for image restoration. *IEEE Transactions on Image Processing*, 15(12):3737–  
793 3748, 2006. 2, 3, 4, 5, 6, 7 828  
794 [23] M. Elad, M. Aharon, and A. Bruckstein. Sparse representation for image restoration. *IEEE Transactions on Image Processing*, 15(12):3737–  
795 3748, 2006. 2, 3, 4, 5, 6, 7 829  
796 [24] M. Elad, M. Aharon, and A. Bruckstein. Sparse representation for image restoration. *IEEE Transactions on Image Processing*, 15(12):3737–  
797 3748, 2006. 2, 3, 4, 5, 6, 7 830  
798 [25] M. Elad, M. Aharon, and A. Bruckstein. Sparse representation for image restoration. *IEEE Transactions on Image Processing*, 15(12):3737–  
799 3748, 2006. 2, 3, 4, 5, 6, 7 831  
800 [26] M. Elad, M. Aharon, and A. Bruckstein. Sparse representation for image restoration. *IEEE Transactions on Image Processing*, 15(12):3737–  
801 3748, 2006. 2, 3, 4, 5, 6, 7 832  
802 [27] M. Elad, M. Aharon, and A. Bruckstein. Sparse representation for image restoration. *IEEE Transactions on Image Processing*, 15(12):3737–  
803 3748, 2006. 2, 3, 4, 5, 6, 7 833  
804 [28] M. Elad, M. Aharon, and A. Bruckstein. Sparse representation for image restoration. *IEEE Transactions on Image Processing*, 15(12):3737–  
805 3748, 2006. 2, 3, 4, 5, 6, 7 834  
806 [29] M. Elad, M. Aharon, and A. Bruckstein. Sparse representation for image restoration. *IEEE Transactions on Image Processing*, 15(12):3737–  
807 3748, 2006. 2, 3, 4, 5, 6, 7 835  
808 [30] M. Elad, M. Aharon, and A. Bruckstein. Sparse representation for image restoration. *IEEE Transactions on Image Processing*, 15(12):3737–  
809 3748, 2006. 2, 3, 4, 5, 6, 7 836